Orbit Determination of Asteroid 2003 HA22

New Mexico Tech Team 7

[a]*Justin Ji, Hyun Kim, Aaron Zhang*

Abstract

The goal of this research was to determine the orbit of Asteroid 2003 HA22 using the Method of Gauss. This involved first taking images of 2003 HA22 at different times by preparing observational requests for several dates. Of the images, we took four of them that had clear images and were preferable for more accurate data collection. After locating asteroid 2003 HA22 from each of the four image sequences, we were able to perform astrometry and photometry on the images with AstroImageJ to extract data of their positions and magnitudes. Using this data, we were able to find the orbital elements of 2003 HA22's orbit using the Method of Gauss. To find the uncertainty of our orbital elements, we used Monte Carlo simulations by changing parameters of our input and modeling the output's spread with a histogram. Using the orbital elements we obtained from the Method of Gauss, we created a 3-D visualization of the orbits of asteroid 2003 HA22 and nearby planets by writing code in VPython. It was found that the Method of Gauss is accurate in calculating the orbital elements of an asteroid and mapping the orbit of the asteroid 2003 HA22 by comparing the results with data from the NASA Jet Propulsion Lab Interface (JPL Horizons).

1. Introduction

Our solar system is covered with countless amounts of space debris, ranging from small fragments of paint from rockets to dead satellites. These space debris can be labeled as natural debris, which are small pieces of meteoroids, or artificial debris, which are debris from man-made objects, such as satellites. [2] Although most of these space debris don't pose a major threat due to burning before making to the Earth's surface, Near-Earth Asteroids (NEAs), which have perihelion distances less than 1.3 AU, are on cosmologists' radar as they threaten to collide with Earth. Of the NEAs, cosmologists pay great attention to Potentially Hazardous Asteroids (PHAs), which have minimum orbit intersection distances less than 0.05 AU and absolute magnitudes less than or equal to 22.0. In our research, we observed NEA 2003 HA22 to improve its orbit calculations and future predictions. Our asteroid can be described with several orbital elements: semi-major axis (a), eccentricity (e), inclination (i), longitude of the ascending node (), argument of perihelion (), and mean anomaly (M0). These orbital elements are parameters that describe an orbit's size, shape, and motion of the asteroid. With three images of the 2003 HA22 taken with the Sun above 30° and minimal moon brightness, we used the Method of Gauss (MoG) to capture its exact location during three roughly evenly spaced periods of time and determine the asteroid's orbit.

2. Observations and Data Analysis

2.1. Observing Requests

Due to the COVID-19 pandemic, observations of 2003 HA22 were done virtually through observation requests submitted to various observatories around the world. Data for observation requests was obtained using JPL Horizons. This information included: right ascension (RA) and declination (DEC) of 2003 HA22, the observable window, and a finding chart of the surrounding region for comparison with reference stars. Our observation requests were submitted to the Cerro Telolo Inter-American Observatory (CTIO), in Vicuña, Coquimbo, Chile for their Prompt-6 Telescope. Once the images were collected, we used AstroImageJ (AIJ) and SAOImageDS9 (DS9) software to analyze our images and calculate the RA and DEC and magnitude of our asteroid. All of our images were taken on the CTIO Prompt-6 telescope and thus the observing strategy was the same for each observation. Using JPL, we found the RA and DEC of 2003 HA22 over the course of its observable window. The observable window was based upon the evening nautical twilight in CTIO and the 30 degree set time of the asteroid, the level in the sky where images are unusable due to poor quality. After the observable window was set, the asteroid motion time was calculated by dividing the camera field of view by two to ensure that the asteroid would be pictured in the middle 25% of the image. The result was converted to arcseconds by multiplying by 60 and then divided by the vertical and horizontal velocity of the asteroid to obtain the asteroid motion times, of which, the lower of the two were taken. If asteroid motion time was less than that of the observable window, a cropped observable window was calculated around transit time, the time when the asteroid was highest in the sky. After this was done, an ephemeris was generated through JPL containing astrometric RA and DECs, apparent azimuth and elevation of 2003 HA22, visual magnitude, and local apparent hour angle.

We list our observations in Table 1.

Table 1:
Team 7 Observation Details

Observation Date (UTC)	Name	MPC Code	Successful?	Comments
06/23/2021	CTIO-Prompt 6	807	N	No Images
06/30/2021	CTIO-Prompt 6	807	Y	
07/06/2021	DSO-14	W38	N	Poor Focus
07/08/2021	CTIO-Prompt 6	807	Y	ONL Data[1]
07/11/2021	CTIO-Prompt 6	807	N	Not Receieved
07/14/2021	CTIO-Prompt 6	807	N	ONL Data[1]
07/18/2021	CTIO-Prompt 6	807	Y	

[1]Data from ONL Team 7

2.2. *Image Reduction*

The images from the observations came in raw (Fig. 1), meaning they contained information that was needed and information that was not. However, the raw images were first validated through AIJ and DS9. After opening the sequence, the RA and DEC from the FITTS header of the first image was compared to the ephemeris generated in the observation request. The first raw image was also compared to the finding chart in DS9 to In order to make the asteroid more observable, the image needed to be reduced. Raw images contain levels of bias and dark current, both of which can be subtracted away using AIJ. Bias level includes read-out noise, digitization noise, and intentional voltage offset while dark current is the accumulation of thermally promoted electrons in the pixels. Raw images are also flat fielded, meaning they usually contain dust donuts and are vignetted. Using AIJ, flat fields can be divided away. [3] This process of subtracting bias level and dark current and dividing away flat fields is known as image reduction.

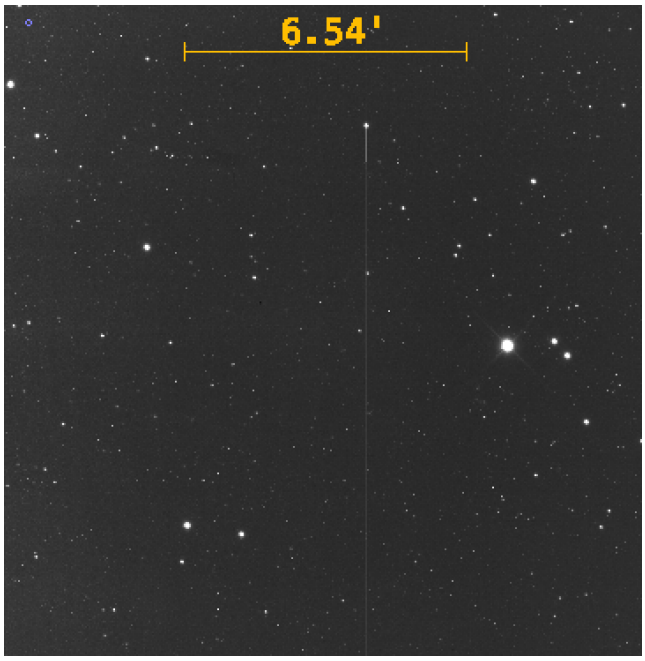

Figure 1: A Raw Image with 2003 HA22 in its Field of View on 06/30/2021

2.3. *Astrometry and Photometry*

Once the image was reduced, astrometry and photometry were performed in order to obtain the RA, DEC, and magnitude of the asteroid. Astrometry is the process finding the RA and DEC of an asteroid by comparing it to the RA and DECs of known reference stars in the area. This is done by dividing the reduced images into three sequences and Plate Solving the first image of each sequence. Plate Solving runs the image through AIJ's database where it identifies reference stars. [1] Once this was done, the RA and DECs of the asteroid and three reference stars were recorded. Photometry is the process of calculating visual magnitude of the asteroid by comparing it with the

same reference stars used in astrometry. Using DS9's USNO UCAC5 star catalog, the RMag and source-sky values of the reference stars were recorded.

$$m_{ast} = m_{star} - 2.5log_{10}(\frac{F_{ast}}{F_{star}})$$

Plugging the magnitude and source-sky values into the above equation, we determined the magnitude of our asteroid for a particular reference star. By averaging this magnitude over all the reference stars, we determined our asteroid's average magnitude. (Table 2)

2.4. Results

Table 2:
Observed RA and DEC of Asteroid 2003 HA22

Observation Date(UTC)	RA	σ_{RA}	DEC	σ_{DEC}	mag	SNR
6/30/2021 00:22:38	15:34:58.34	5.90e-06	-13:43:33.4	4.56e-06	17.413	12.12
6/30/2021 00:51:35	15:35:01.06	5.00e-06	-13:43:53.2	4.78e-06	17.411	13.66
6/30/2021 01:13:34	15:35:03.09	4.59e-06	-13:44:09.5	3.97e-06	17.257	12.81
7/08/2021[1] 00:22:38	15:58:49.66	3.08e-06	-16:15:08.7	3.18e-06	16.916	14.16
7/08/2021[1] 00:51:35	15:58:55.32	4.62e-06	-16:15:45.4	1.65e-06	17.014	15.25
7/14/2021[1] 02:25:29	16:21:50.20	5.30e-06	-18:21:51.8	3.52e-06	16.862	15.68
7/14/2021[1] 02:45:24	16:21:53.39	4.12e-06	-18:22:08.4	3.08e-06	16.888	15.67
7/14/2021[1] 03:04:43	16:21:50.39	3.38e-06	-18:21:51.8	2.48e-06	16.784	15.21
7/18/2021 02:25:24	16:38:44.95	4.85e-06	-19:43:06.0	5.42e-06	16.618	9.59
7/18/2021 02:45:19	16:38:48.83	5.03e-06	-19:43:25.6	5.42e-06	16.696	14.22
7/18/2021 03:04:38	16:38:51.81	4.28e-06	-19:43:40.3	5.11e-06	16.766	9.59

3. Orbit determination and Visualization

3.1. Methods

After performing astrometry and photometry on three images, we obtained the time and equatorial coordinates of our asteroid. Then, we used the iterative process of Method of Gauss (MoG) to determine our asteroid's approximate heliocentric position and velocity vectors. From the position and velocity vectors, we calculated the 6 orbital elements.

Before we iterated through MoG to obtain precise positions and velocity vectors, we first needed to calculate initial vectors. Due to conservation of angular momentum, all three position

[1]Data from ONL Team 7

vectors must be in the same plane, and thus we could express the position vector of the second observation as a linear combination of the position vectors of the first and third observations. By defining the vectors in terms of one another and using the fundamental triangle, we can express the range to the asteroid with the scalar equations of range.

However, the scalar equations of range require the c's and D's terms, which in turn require the f's and g's. If we had the orbital elements, we could easily solve for f and g. Since we do not, we expressed the position vector with a Taylor series expansion, determining the first few terms of the f and g series. We truncated the Taylor series to just the terms that don't require the position or velocity vectors, then solved for approximate f and g coefficients. Finally, we obtained an approximation for f and g, and could backtrack to obtain an approximation of the position and velocity vectors.

Next, we iterated using our initial position and velocity vectors to obtain more accurate vectors. By looping until the differences in ranges no longer surpassed a small number, we could repeatedly calculate new c, rho, position, and velocity vectors. Additionally, because we have preliminary values for position and velocity, we can use the exact f and g function definitions instead of the Taylor series approximations. These functions themselves depend on an iterative loop to calculate the eccentric anomaly, so our code contains two iterative loops.

Once we calculated our precise position and velocity vectors, we substituted them into equations 59, 61, 62, 64, 65, and 80, [6] to solve for the semi-major axis, eccentricity, orbit inclination, longitude of ascending node, argument of perihelion, and mean anomaly, respectively. These were the final orbital elements from our observations. We then set out to determine the means and standard deviations of the orbital elements using Monte Carlo simulations.

Attempting to find the uncertainty of the orbital elements mathematically is not feasible due to the immense number of operations that go into the calculation of every element. Instead, we slightly change the input right ascensions and declinations of our three observations and calculate the corresponding orbital elements. By sampling a large number of times, we obtain a distribution of each orbital element and can determine the mean and standard deviation of each distribution.

Additionally the visualization of the inner planets and our asteroids (Fig 8) was done using our Orbit.Viz code. The orbital elements of the planets and asteroids were taken from JPL Horizons for consistency.

3.2. Results

After calculating our orbital elements, we also verified whether or not the orbital elements accurately predicted the asteroid's position from data not in our MoG solution. This was done by taking the orbital elements calculated from the first three observations and generating an ephemeris at the time and location of the fourth observation, essentially doing the reverse of the Method of Gauss. The RA and DEC calculated were approximately 1 degree and 5 degrees off respectively. Therefore, the orbital elements do accurately predict the asteroid's position.

We see from our calculated orbital elements that the semi-major axis is 2.069 AU, eccentricity is 0.448, inclination is 1.734 degrees, longitude of the ascending node is 120.910 degrees, argument of perigee is 165.313 degrees, and the mean anomaly is 3.173 degrees. Using these orbital elements, we can calculate its perihelion (q). Using the equation $q = a(1 - e)$, we find that $q = 2.069 \cdot (1 - 0.448) = 1.142\ AU$. As a result, because the asteroid has a semi-major axis

greater than 1AU and a perihelion between values 1.017AU and 1.3AU, the 2003 HA22 can be classified as an Amor, which matches its classification in published conclusions. [5] According to the data we obtained, the 2003 HA22 is not a potentially hazardous asteroid (PHA) because it has an absolute magnitude less than 22 and a minimum orbit intersection distance (MOID) greater than 0.05 AU.

In Table 3, we see that our values of orbital elements are similar to that found from JPL Horizons to approximately 1 degree, but unfortunately do not fall within the range of uncertainty calculated in our Monte Carlo (Table 4). For example, we calculated the semi-major axis to be 2.069 AU, while JPL Horizons calculated the semi-major axis to be 1.876 AU, with the Monte Carlo uncertainty range being +/- 0.03 AU from 1.86 AU. A possible reason for the discrepancy is either an error in our Monte Carlo code or an error in calculating the orbital elements.

Table 3:
Comparison of Orbital Elements of Asteroid 2003 HA22

	a (AU)	e	I (degrees)	$\Omega(degrees)$	$\omega(degrees)$	M (degrees)
NMT Team 7	2.069	0.448	1.734	120.910	165.313	3.173
JPL Horizons	1.876	0.395	1.609	121.789	163.510	4.272

Table 4:
Uncertainties of Orbital Elements of Asteroid 2003 HA22

	σ_a (AU)	σ_e	σ_I (degrees)	σ_Ω (degrees)	σ_ω (degrees)	σ_M (degrees)
NMT Team 7	0.03	0.01	0.03	0.09	0.05	0.12

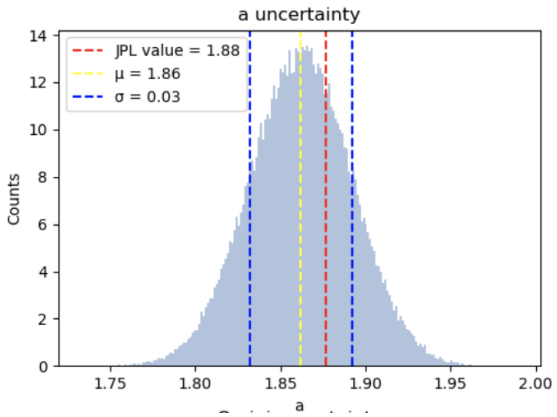

Figure 2: Uncertainty of a

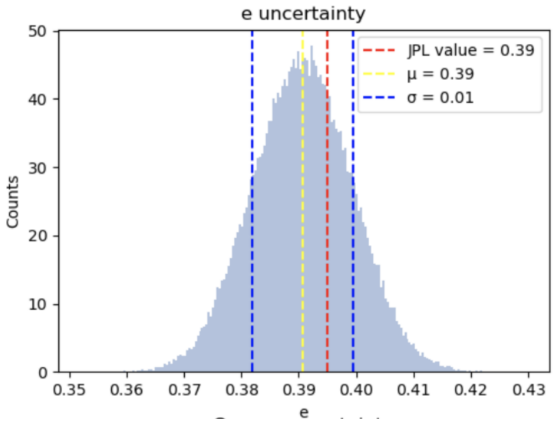

Figure 3: Uncertainty of e

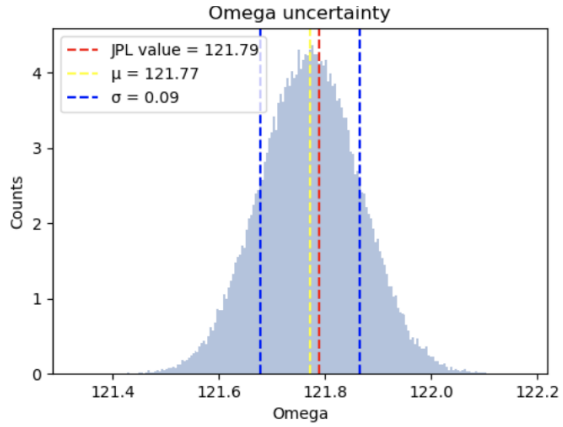

Figure 4: Uncertainty of Ω

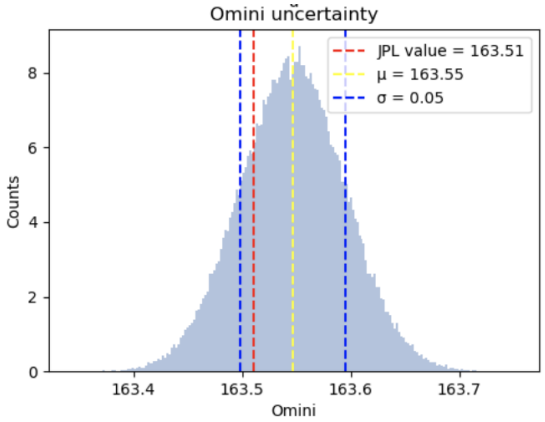

Figure 5: Uncertainty of ω

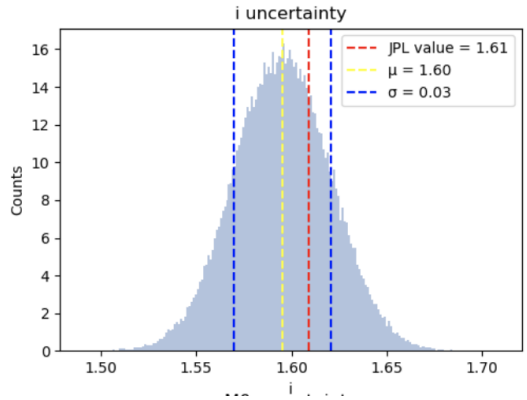

Figure 6: Uncertainty of i

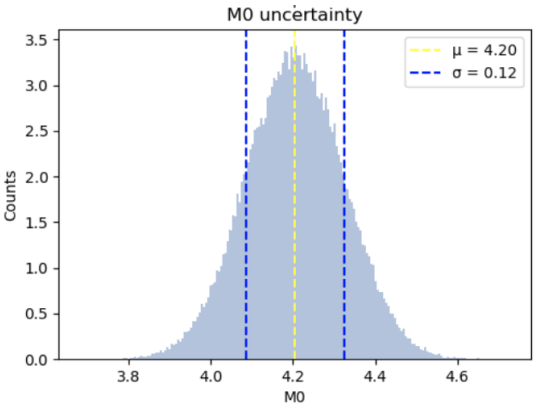

Figure 7: Uncertainty of $M0$

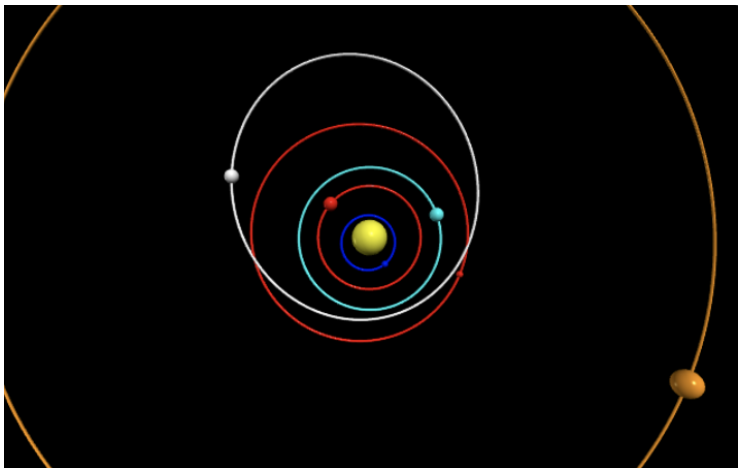

Figure 8: Visualization of the Planets Within the Asteroid Belt

4. Discussion

To predict the long-term behavior of asteroid 2003 HA22, we made 15 asteroid clones by slightly altering the 5th and 6th decimal points of position and velocity vectors, and found their individual fates by running the program Swift. As shown in Figure 9, we found that 3 of 15 particles (20%) were discarded and predicted to have too small a perihelion (Fig 10) ,which means they will end up too close to the Sun, while 12 of 15 particles (80%) were discarded and predicted to end up too far from the Sun (Fig 11). We also found from our data that 2 of the 15 particles (13%) will last encounter Earth before getting too close to the Sun.

It can be seen in Figure 10 that test particle 14 will be discarded due to having too small a perihelion, or coming too close to the Sun. We see that the blue line in Figure 11, the perihelion, approaches 0 as time approaches about 5.2 million years. In Figure 11, we see that the perihelion and aphelion suddenly increases near 0.014 million years to 600AU and 1200AU, respectively, which is expected of a discarded particle too far from the Sun.

Another member emulated the same process but altered different numbers and found that 1 particle (7%) had an issue in integrating the orbit and was thus discarded. 1 particle's (7%) orbit became too far from the sun, 7 particles (47%) had a perihelion too small a perihelion, 1 particle (7%) last encountered Venus and 3 last encountered Earth (20%). 2 out of 15 (13%) of his asteroid particles remained active after 50 million years (mya). An example of an active particle can be seen in Figure 12 where the particle's aphelion oscillated between 1.2 and 3.0 AU, and the perihelion oscillated between 0 and 1.2 AU.

Discarded Particles : 15 out of 15

#	why?	Last pl encountered	a	q	Q	i
1	-4	3	2.0055	0.0046	4.0064	18.7148
2	-4	3	2.4970	0.0046	4.9893	54.1502
3	-3	0	0.5286	-1.8793	2.9364	0.9905
4	-3	0	0.1313	-4.1753	4.4379	179.3006
5	-3	0	0.0928	-2.2419	2.4276	2.5059
6	-3	0	0.0306	-5.1331	5.1944	0.4229
7	-3	0	0.2127	-4.2683	4.6936	0.9724
8	-3	0	0.0306	-6.1339	6.1951	0.5585
9	-3	0	0.0378	-4.0618	4.1374	0.5772
10	-3	0	0.0479	-7.1872	7.2831	0.5878
11	-3	0	0.0491	-0.2098	0.3080	7.4353
12	-3	6	0.0377	-8.0568	8.1321	0.3686
13	-3	0	0.0478	-5.1651	5.2608	0.7407
14	-4	4	2.4161	0.0033	4.8288	32.2783
15	-3	5	628.5465	5.6051	1251.4878	20.6977

Fate of Discarded Particles :

```
    0 have istat(i,2) = -1  ==> Danby did not converge
    0 have istat(i,2) = -2  ==> Ejected from the system
   12 have istat(i,2) = -3  ==> Too far from the Sun
    3 have istat(i,2) = -4  ==> Too small a perihelion
    0 have istat(i,2) =  1  ==> Too close to the Sun
    0 have istat(i,2) =  2  ==> Too close to planet 2
    0 have istat(i,2) =  3  ==> Too close to planet 3
    0 have istat(i,2) =  4  ==> Too close to planet 4
    0 have istat(i,2) =  5  ==> Too close to planet 5
    0 have istat(i,2) =  6  ==> Too close to planet 6
    0 have istat(i,2) =  7  ==> Too close to planet 7
    0 have istat(i,2) =  8  ==> Too close to planet 8
  ---
   15/  15
```

Figure 9: Fate of Discarded Particles from Student 1's Orbit Integration Research

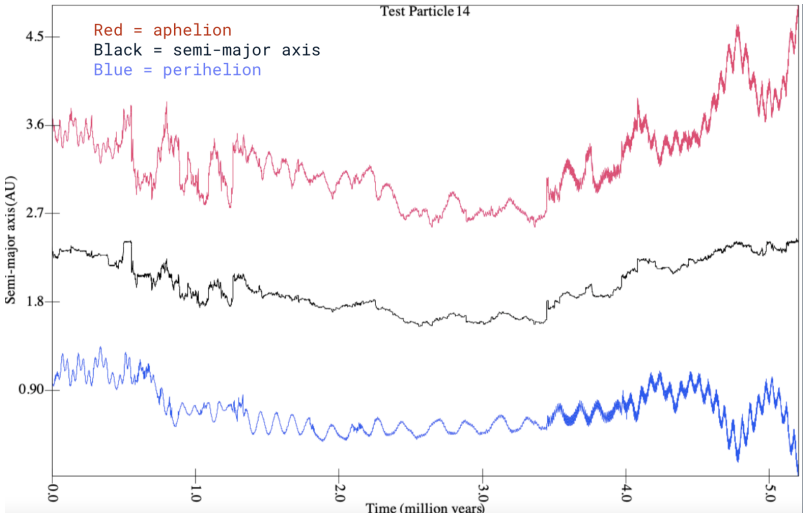

Figure 10: Example of a Test Particle with Too Small a Perihelion

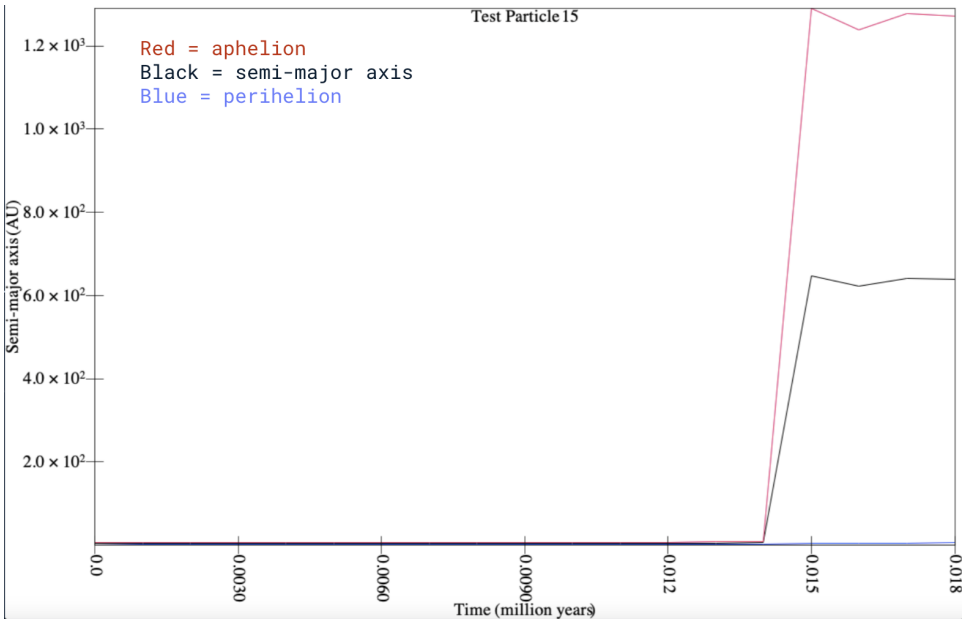

Figure 11: Example of a Test Particle with Too Far a Perihelion

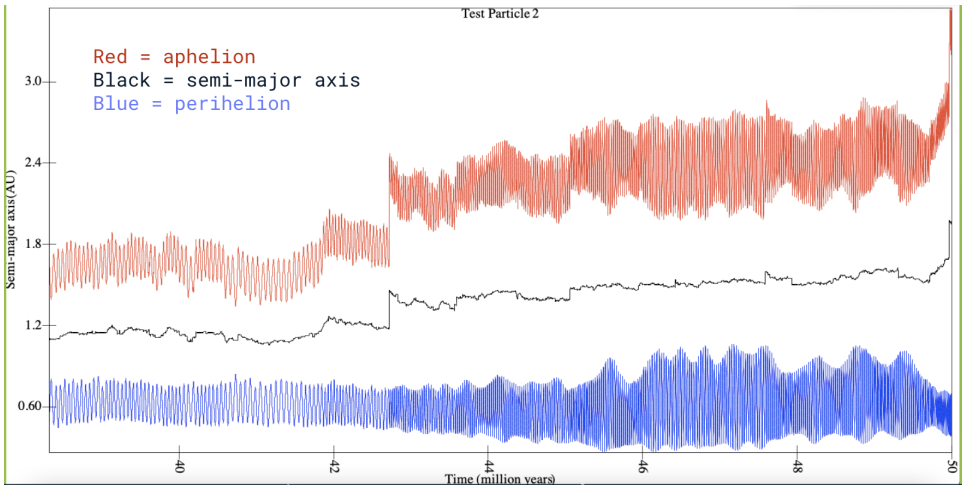

Figure 12: Example of a Test Particle That Survived

We conclude from these data that it is fairly likely asteroid 2003 HA22 will end up too far from the Sun. Also, we predict it will be unlikely 2003 HA22 will collide with Earth with its calculated probability about 13% to encounter Earth in the next 50 million years.

5. Reflection

In summary, Team 7 was able to accomplish the goal of determining the orbit of Asteroid 2003 HA22 by employing the Method of Gauss. We were able to locate the asteroid from our observations and after reducing the images and performing astrometry and photometry. Then, we calculated the orbital elements and performed a Monte Carlo on the results and also produced a visualization of the orbits of the planets within the asteroid and 2003 HA22. Our calculated orbital elements did not fall within the uncertainty range calculated by our Monte Carlo. This could be attributed to either error in our Monte Carlo code or error in calculating the orbital elements.

During our time at SSP, our group had to work around the time frame set for us. Due to having only 5 weeks, a relatively short period of time, days with uncooperative weather, and sudden telescope location changes, there were not that many chances to obtain data. Our group only had time to submit four observing requests, with two of them resulting in unusable data. Thus, if this research was replicated, one piece of advice our group has for our colleagues would be to make sure that they have enough data to work with. Another piece of advice our group has would be to try to observe through different telescopes. Because we had to submit observing requests according to the observing schedule, there was no way to prevent factors like poor weather or illumination percentage of the moon from hindering our data collection. Thirdly, we would advise to perform astrometry and photometry at the same time. This would avoid having stars in JPL not show up in the catalog in DS9. Finally, our group encourages collaboration, as often, positive collaboration results in increased efficiency and enhanced knowledge for everyone.

6. Acknowledgements

We would like to thank Dr. Rengstorf, Dr. Andersen, and Dr. Bauer for teaching us the Method of Gauss and preparing us for this report. None of what we did at SSP would have been possible had they not taught us. We would also like to thank the teacher assistants, Abby, Tristan, Katie, and Michael for their unwavering support and willingness to take the time to help us understand the material. Thirdly, special thanks goes to ONL Team 7, who let us use their raw images on 07/08/2021 and 07/14/2021. We would not have had enough data had not been so kind and given us permission to do so. Finally, we would like to thank Ms. Belote and Ms. Martinez for ensuring that operations at SSP run smoothly so students like us get to have an experience of a lifetime!

7. References

References

[1] Fallscheer, C. (Author) (2021) *Asteroid Astrometry Data Reduction Procedure*.
[2] FAST FACTS ON SPACE DEBRIS,
`https://www.spaceacademy.net.au/watch/debris/sdfacts.htm`
[3] Rengstorf, Adam. (Author) (2021)
`Cameras and Images`
[4] HORIZONS Web-Interface,
`ssd.jpl.nasa.gov/horizons.cgi`
[5] Neo Basics,
`https://cneos.jpl.nasa.gov/about/neo`$_g$*roups.html*
[6] Rengstorf, Adam, and William Andersen. (Author) (2021) *Orbit Determination Packet*.